

Wall Shear Stress Measurements in a Shock-Wave Boundary-Layer Interaction

V. Sreedhara Murthy* and W. C. Rose†

NASA Ames Research Center, Moffett Field, Calif.

Detailed measurements of wall shear stress (skin friction) were made with specially developed buried wire gages in the interaction regions of a Mach 2.9 turbulent boundary layer with externally generated shocks. Separation and reattachment points inferred by these measurements support the findings of earlier experiments which used a surface oil flow technique and pitot profile measurements. The measurements further indicate that the boundary layer tends to attain significantly higher skin-friction values downstream of the interaction region as compared to upstream. Comparisons between measured wall shear stress and published results of some theoretical calculation schemes show that the general, but not detailed, behavior is predicted well by such schemes.

Nomenclature

- b = span of the sensor
 C_f = skin-friction coefficient = $\tau_w / \frac{1}{2} \rho_\infty U^2_\infty$
 k = coefficient of thermal conductivity of flow medium at sensor operating temperature
 k_{sub} = coefficient of thermal conductivity of substrate material
 ℓ = length of the sensor in stream direction
 M = freestream Mach number
 Nu = Nusselt number for sensor = $(q - q_0) / bk(T_w - T_0)$
 Pr = molecular Prandtl number of flow medium
 p = pressure
 q = total heat loss rate from sensor in flow
 q_0 = heat loss rate from sensor in absence of flow
 Re_δ = boundary-layer thickness Reynolds number = $\rho_\infty U_\infty \delta / \mu_\infty$
 T_0 = sensor temperature when sensor is not operating
 T_w = sensor temperature when heated (operating)
 u = velocity
 x = streamwise coordinate
 α = shock generator setting (see Fig. 1)
 δ = boundary-layer thickness
 λ = equivalent length factor (determined by calibration)
 μ = absolute viscosity of flow medium at sensor operating temperature
 μ_∞ = absolute viscosity of flow medium at freestream conditions
 ρ = density of flow medium at sensor operating temperature and local pressure
 ρ_∞ = density of flow medium at freestream conditions
 τ_w = wall shear stress

Subscripts

- sub = pertaining to substrate
 t = total or stagnation conditions
 w = conditions at wall
 ∞ = freestream conditions upstream of incident shock

Introduction

ONE of the most important and still unsolved problems in fluid mechanics is the interaction between a shock wave

Presented as Paper 77-691 at the AIAA 10th Fluid and Plasodynamics Conference, Albuquerque, N. Mex., June 27-29, 1977; submitted July 22, 1977; revision received March 6, 1978. Copyright © American Institute of Aeronautics and Astronautics, Inc., 1977. All rights reserved.

Index categories: Boundary Layers and Convective Heat Transfer—Turbulent; Supersonic and Hypersonic Flow.

*Senior NRC Research Associate.

†Research Scientist. Member AIAA.

and turbulent boundary layer.¹⁻³ The interaction field is a strong function of Reynolds number, boundary-layer thickness, and pressure gradient. Even when it is possible, real-flight-equivalent simulation of these variables in ground-based test facilities is expensive. This has led to the development of detailed numerical simulations of such flowfields. Progress in such simulations, however, has been inhibited by lack of sufficient experimental data that can lead to the definition of a turbulence model acceptable to interaction flowfields.^{4,5} One parameter that plays an important role in turbulence modeling is the wall shear stress⁴ and it is toward the study of this parameter that the present investigation is directed.

Accurate wall shear stress measurements in shock-wave boundary-layer interaction regions have not been possible so far because of the lack of nonintrusive measurement techniques. Surface pressure probes such as Preston probes and Stanton probes, because of their protrusion beyond the wall surface, cause disturbances to boundary-layer flow that not only raise doubts about the reliability of such measurements but also make it almost impossible to measure downstream stations simultaneously. Besides, their calibrations are difficult and unreliable in regions with large streamwise pressure gradients. Floating element balances are relatively large and their calibrations in a region of pressure gradient are uncertain because of the buoyancy effects on the sensing elements. And boundary-layer pitot profile

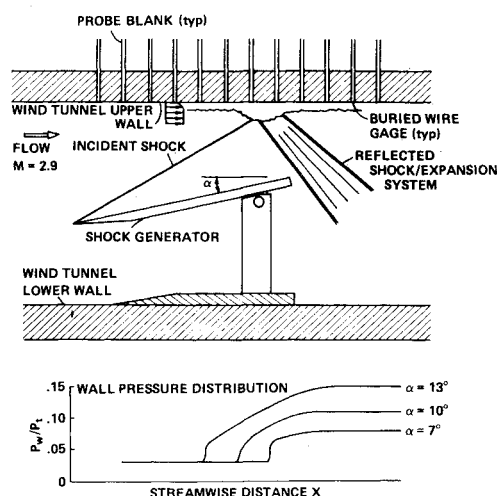


Fig. 1 Schematic of experimental apparatus and surface pressure distribution.

measurements, primarily for obtaining skin friction, are impractical in most situations. This leaves only the heated flush-sensor technique, which had its origin long ago⁶ but failed to gain popularity as an effective technique, at least on a par with other conventional wind-tunnel measurement techniques, until recently.⁷

The heated sensor technique relies on the analogy between heat transfer and momentum transfer in a portion of the boundary layer closest to the wall. The sensor can be made small enough so that it responds to a very thin flow layer close to the wall and thus achieves a calibration independent of the status of the boundary layer, whether laminar or turbulent.⁷ These sensors usually take the form of a slender wire or thin metallic film which is flush-bonded over its entire span to the surface of a low thermal conductivity substrate with embedded electrical leads at each end. The gage is mounted such that the sensor becomes flush with the surface where skin friction is to be measured. Heat loss from the sensor due to boundary-layer flow over it then becomes a function of local skin-friction and pressure gradient.⁸ It is usually convenient to operate the sensor in a constant temperature mode through an anemometer system.

Several investigators have used this technique in the past, but their efforts were largely confined to an examination of the calibration characteristics.⁸⁻¹² Even so, the results of their investigations, as described in the published literature, do not lead to any firm recommendations about the best method of making gages for use on wind-tunnel models. Sputtered film gages on quartz or glass substrates, which are more typical of the gages used by earlier investigators, offer low sensitivity in terms of skin-friction measurements because of their high conduction heat loss into the substrate. Besides, these types of gages are not really well suited for arranging instrumentation on wind-tunnel models where, to avoid surface roughness, built-in gages may be preferred to implantable ones. An alternative to sputtered film gages is to flush-bury wires in a substrate⁷ and use them as the heated sensors. The present investigation, for the most part, concerns such gages.

The interaction flowfield selected for study in the present investigation (see Fig. 1) consists of a wedge-generated shock impinging on the wall boundary layer of a $M=2.9$ supersonic wind tunnel. The experimental apparatus is the same as the one used by Reda and Murphy.¹³ This flow has earlier been documented through detailed pressure and pitot profile measurements by Reda and Murphy and through laser velocimetry measurements by Modarress and Johnson¹⁴ and Bachalo et al.¹⁵ Present measurements supply the distribution of wall shear stress in the interaction region and thus significantly increase the data base on which flow modeling may be carried out. Analytical treatments of this flow may be found in Refs. 16 and 17.

Gage Construction

Apart from the choices of sensor and substrate materials that might distinguish different gages, there exist different methods of making such gages, and the construction techniques appear to be appropriate for classifying the gages. In all types of gages used in the present series of experiments, the electrical leads were thin nickel wires inserted into holes in the substrate material and firmly epoxied in place.

Adhesive-Cast Gages

The sensor wire is spot-welded to the electrical leads; a soft swab is used to apply an adhesive to the whole of the substrate surface. The adhesive is then allowed to cure with the surface gently pressed against a nonbondable surface so that the cured adhesive may reproduce the original contour of the substrate surface. The gage surface is finally polished to just expose the top of the wire. This technique is essentially that discussed by Rubesin et al.⁷ In the present investigation, gages of this type were made with platinum-rhodium wires and tungsten wires as sensors, Rexolite (a cross-linked styrene copolymer) and

polystyrene as substrates, and Rexolite adhesive and polyester casting resin as adhesives. A teflon sheet was used as the nonbondable mating surface. The adhesive in this case was cured in a furnace for several hours at elevated temperatures.

Heat-Buried Gages

Again, the sensor wire is spot-welded to the electrical leads flush with the substrate surface. The wire is buried by gently pressing it against the substrate as it is heated by a dc power supply to a temperature slightly in excess of the softening temperature of the substrate material. The surface is then polished to just expose the top of the wire. The sensor and substrate materials for the gages used in the present investigation were the same as that for the adhesive-cast gages.

Film Gages

The sensor is deposited in the form of a thin narrow strip by a vacuum sputtering or similar technique across flush-embedded electrical leads on a well-polished substrate. A protective coating is usually applied over such films. This method is generally not easily workable for all types of sensor and substrate materials. Gages of this type are, however, commercially available in the form of nickel or platinum film on quartz or polyimide-substrate. TSI (Thermo-Systems Inc., St. Paul, Minn.) Model 1237 gages with platinum films protected by quartz coating on quartz substrate were used in this study.

Solvent-Buried Gages

The sensor wire is spot-welded to the electrical leads and flush with the substrate surface such that the wire lies flat on the surface. A soft swab is then used to apply a highly volatile solvent, capable of dissolving the substrate material around the wire so that the solvent dissolves the adjacent substrate material and causes it to deposit over the wire. As the solvent evaporates, a thin layer of substrate material forms around the wire and firmly holds it on the substrate surface. With this technique it is possible to make the substrate coating very thin compared to the wire cross section and thus reduce any frequency response or sensitivity problems. The coating on top of the wire could be left as is or polished away. It has proved best to leave the coating on, as it protects the wire and also because it eliminates what might be a rather unimportant fabrication step, to bring a closer similarity between gages with identical sensor cross sections. Because of the small sensor wire dimensions ($5-10\ \mu$ in diameter), any extra fabrication step, no matter how skillfully executed, always tends to induce dissimilarities in otherwise similar gages. Most of the gages used in the present investigation were of this type;

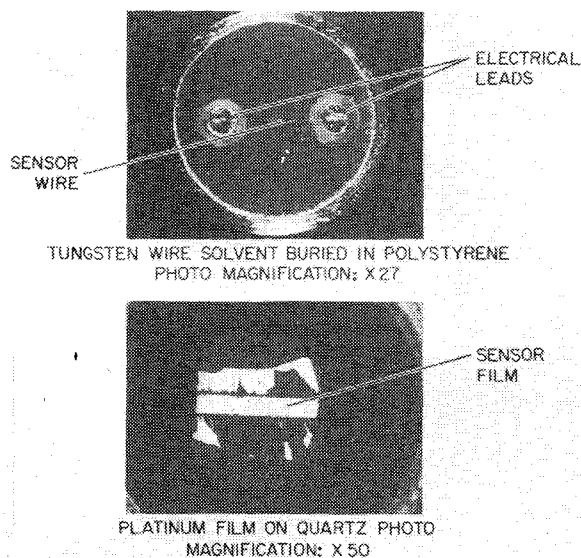


Fig. 2 Photographs of typical gages, 60% reduction.

platinum-rhodium wires were used as sensors, polystyrene as substrate, and methyl-ethyl-ketone as solvent.

Thirty-five gages, representative of all the aforementioned types, were made. Photographs of typical gages are shown in Fig. 2. Measurements of surface waviness on typical gages revealed that the solvent-buried gages, which are apt to possess larger waviness as compared to other gages (because of the way they are made), were still less than 4μ . The following sections describe the calibration and use of these gages to measure directly the skin friction distribution in shock-wave-turbulent boundary-layer interaction regions.

Gage Calibration

Calibration of heated flush-mounted film or wire sensors for measurement of skin friction is based on the relationship between heat-transfer rate from the sensor, local skin friction, and pressure gradient. An expression for this relationship, given by Brown,⁸ can be written as:

$$\frac{\rho \tau_w (\lambda l)^2 Pr}{\mu^2} = 1.9 Nu^3 - 0.2778 \frac{\rho (\lambda l)^3 Pr}{\mu^2} \frac{dp}{dx} \frac{l}{Nu} \quad (1)$$

It may be shown from classical heat conduction theory that the no-flow heat-transfer rate q_0 (which appears in the definition of Nu) for a wire submerged in any medium must be proportional to the product $bk_{sub}(T_w - T_0)$. Calibration of any gage would therefore imply determination of the no-flow heat loss factor $q_0/bk_{sub}(T_w - T_0)$, and the equivalent length factor λ . During operation, the gage face temperatures are inferred from the sensor's unheated resistance, thus requiring an additional calibration step to determine the sensor resistance temperature characteristics. The no-flow heat loss factor (i.e., the "conduction loss") is evaluated from measurements in still air and the equivalent length factor is obtained from a measurement in a boundary layer with known wall shear stress.

This approach to calibrating different gages through still-air tests and a single measurement in a known boundary-layer flow assumes a linear relationship between Nu and $\tau_w^{1/2}$ terms in Eq. (1). This assumption derives experimental support from the many detailed calibration tests reported in the literature. In almost all of the reported cases, the sensor dimensions are small enough so that one can simply neglect the term involving pressure gradient in the calibration law [Eq. (1)]. Bellhouse and Schultz^{9,10} have shown that flush-mounted hot film gages may be used to measure skin friction in both laminar and turbulent boundary layers with errors less than 5% for a two-point calibration. Tests reported by Brown⁸ demonstrate that the calibration law, Eq. (1), is fully justified. Owen and Bellhouse¹¹ and Rubesin et al.⁷ also found their calibration to fit the same law. Unfortunately, these references have not given the no-flow heat loss characteristics appropriate to still-air conditions, thus making it impossible to check whether such no-flow heat loss would agree with the intercept of the calibration curve at the zero skin-friction value.

McCroskey and Durbin¹² did measure the conduction loss and concluded that their calibrations follow Eq. (1), but that the zero skin-friction intercept of the calibration curve is greater than the directly measured conduction loss by about 6 to 10%. There are simply not enough data to determine whether this feature is peculiar to the type of gage used by them or whether this might be a universal characteristic of this kind of gage. Their gage had effectively two nonsimilar substrate layers below the sensor and further required the approaching flow to endure a fair measure of surface roughness built up by the backing plastic film and the bonding cement. In any case, the disparity is not prohibitively large and is perhaps within the observed scatter in typical calibration tests. The present authors assume for simplicity that any disparity between zero skin-friction intercept of

calibration curve and still-air heat loss tests is within experimental uncertainty.

Experiment

The tests were conducted in the 20.32 cm \times 20.32 cm, variable Mach number, supersonic wind tunnel of the NASA Ames Unitary System. Freestream Mach number was 2.9, tunnel total pressure was 6.80 atm (100 psia), and tunnel total temperature was about 290 K. Earlier¹³ measurements with free test sections have shown that the upper wall boundary layer has a thickness of 1.7 cm and a thickness Reynolds number of 0.97×10^6 . The tunnel can be run continuously.

A schematic of the test apparatus is shown in Fig. 1. The shock generator is a sharp leading edge, full-span flat plate with independently variable incidence and axial location settings. The shock generated by the wedge impinges on the upper wall boundary layer to produce the interaction under study. Buried wire gages arranged on the end faces of 3.2-mm-diam probe blanks were mounted in the probe opening of an upper wall insert block and held securely in place so that sensor faces of the gages became flush with the flow surface. A more detailed account of the apparatus and flow documentation is given in Ref. 13.

The gages were operated in the constant temperature mode through an anemometer system. Operating temperatures of the sensors were maintained at about 60°C in order to avoid any problem that might result from the softening of substrate materials at higher temperatures. Gage calibrations were

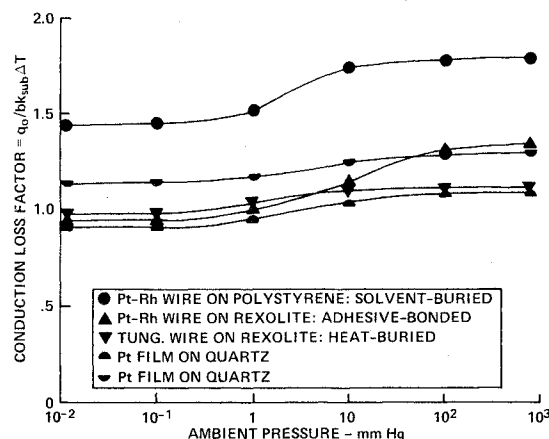


Fig. 3 Conduction loss characteristics of buried wire gages at different ambient pressures.

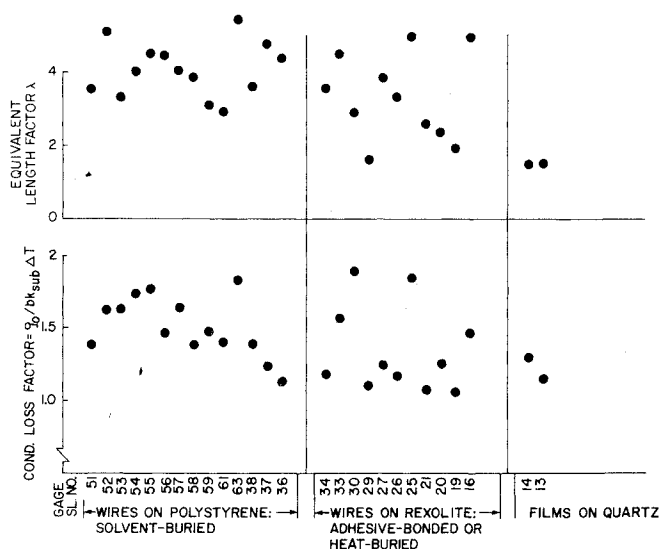


Fig. 4 Calibration constants of different gages used in the present test series.

achieved by first running them under still-air conditions to obtain the no-flow heat loss factor ($q_0/bk_{\text{sub}}(T_w - T_0)$) and then making measurements with a known flow in test section¹³ to obtain the equivalent length factor λ .

Three different shock generator incidence settings, namely $\alpha = 7$ deg, $\alpha = 10$ deg, and $\alpha = 13$ deg, were used in the present series of tests corresponding to unseparated, slightly separated, and fully separated boundary layers. The 13-deg case was severe enough to cause an extensive separated region followed by reattachment and recovery in a near-zero pressure gradient. For any given incidence setting, the shock generator was translated in step increments along the flow direction so as to vary the position of the shock in relation to the fixed locations of the gages. This allowed measurements to be made at any desired fine spacing in the interaction region.

Results and Discussion

The results of no-flow heat loss tests in still-air conditions at different ambient pressure levels are shown in Fig. 3. It may be seen that the no-flow heat loss factor remains practically unchanged at pressure levels above 0.02 atm due to natural convection at the higher pressures. Since the 0.02-atm pressure level is below that usually encountered in aerodynamic wind-tunnel testing, one does not need to consider these pressure level effects, per se. Fig. 4 shows the conduction (no-flow) heat loss factors and the calibrated equivalent length factors for the different gages used in this test series. In spite of the care taken to fabricate identical gages, the calibration constants were not identical. The reason for the difference among various gages is not evident at the time, although the method by which the sensor is bonded to the substrate might allow variations in thermal contact resistance and coating thickness as well as end effects at the electrical leads. However, there are no measurable changes in the calibration constants with either thermal cycling or sustained use. These variations among individual gages strongly suggest that the gages need to be calibrated individually to achieve accurate results. The next obvious step is to examine whether any strong correlation exists between the two calibration constants, as one might expect for gages of the same type. If such a correlation were to exist, the whole task of calibration would reduce simply to the determination of the no-flow heat loss factor. An effort in this direction is shown in Fig. 5; the figure shows that the correlation, if any, is rather weak and cannot be used for accurate measurements. It is important to establish the fact that the present gages have a very low conduction loss and, hence, have the potential for increased accuracy for making quantitative skin-friction measurements. Figure 6 compares the calibration characteristics reported by other investigators with the calibration curves of a few gages typical of those used in the present series. It is clearly evident that the present gages with Rexolite and polystyrene substrates are equal to the best previously investigated.

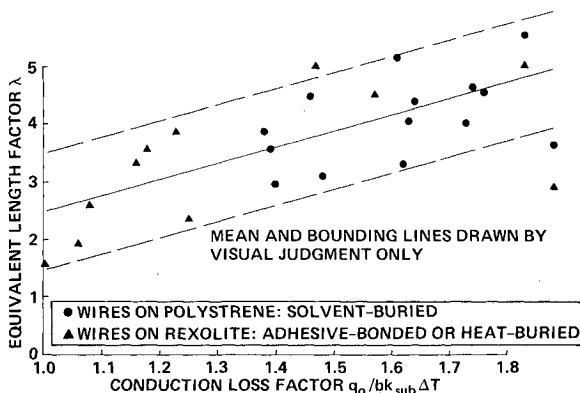


Fig. 5 Correlation between calibration constants of buried wire gages.

With regard to the relative merits of different types of gages, it was found, through sustained operation in typical flow situations, that the solvent-buried gages were more reliable and lasted longer than others. Gages with sensor wires exposed to the flow medium appeared to undergo calibration changes and in most cases ultimately failed. Commercially available gages with platinum film sensors protected by quartz coating are quite rugged but are somewhat insensitive because of their high no-flow heat loss. Besides, such film gages have effective lengths (λl) much larger than wire gages of approximately the same electrical resistance and, therefore, become subject to much larger pressure-gradient-based corrections in typical applications.

Skin-friction distribution measured for the shock generator setting of 7 deg is shown in Fig. 7; the result of earlier pitot pressure profile measurements (unpublished data) is converted to skin-friction values using the method developed by Rubesin et al.⁴ Also shown in Fig. 7 is the result of calculations that used a relaxation model¹⁶ for turbulent shear stress in the boundary-layer code developed by Murphy and Davis.¹⁸ It is seen that the present data and other data reproduced here agree only with regard to the general trend; they fail to agree in terms of actual skin-friction values, especially downstream of the interaction region. Present data show that the boundary layer attains significantly higher skin-friction values downstream of the interaction region.

Figure 8 presents the measured rms values of the output voltage signal normalized with respect to flow-based signal strength. This shows that the rms value increases gently through the interaction region, implying a mild interaction.

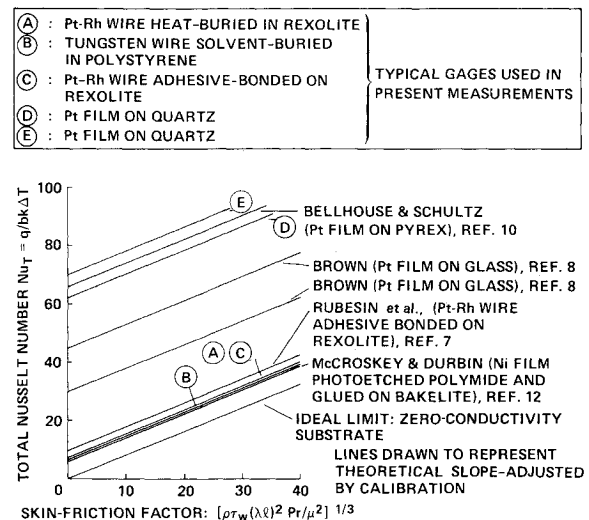


Fig. 6 Calibration of heated sensor gages.

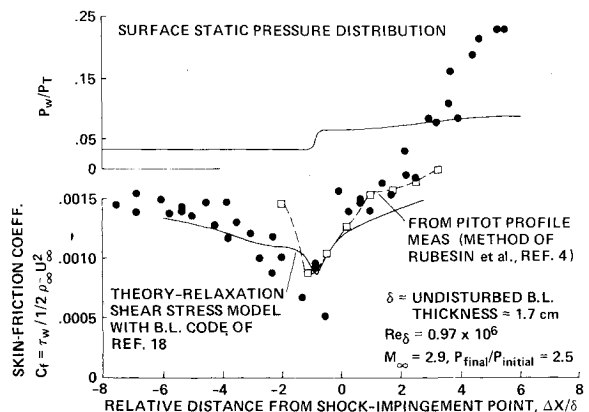


Fig. 7 Skin-friction distribution for $\alpha = 7$ deg, $M_\infty = 2.9$, $P_{\text{final}}/P_{\text{initial}} = 2.5$.

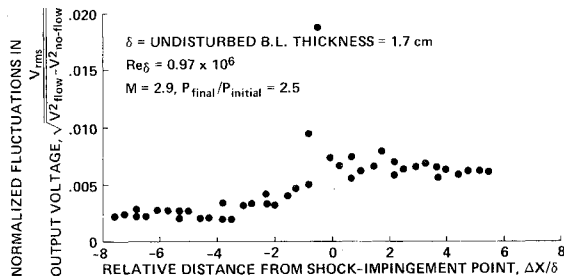


Fig. 8 Normalized fluctuations in gage outputs within interaction region, $\alpha = 7$ deg, $M_\infty = 2.9$, $p_{final}/p_{initial} = 2.5$.

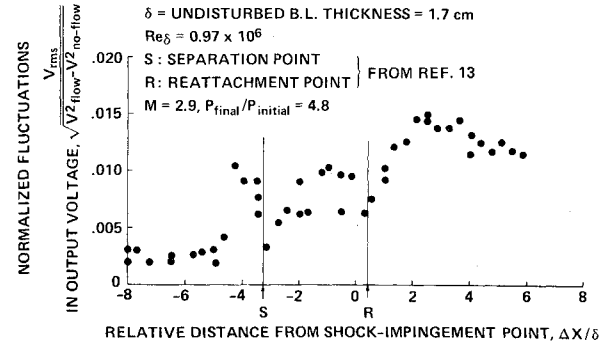


Fig. 10 Normalized fluctuations in gage outputs within interaction region, $\alpha = 13$ deg, $M_\infty = 2.9$, $p_{final}/p_{initial} = 4.8$.

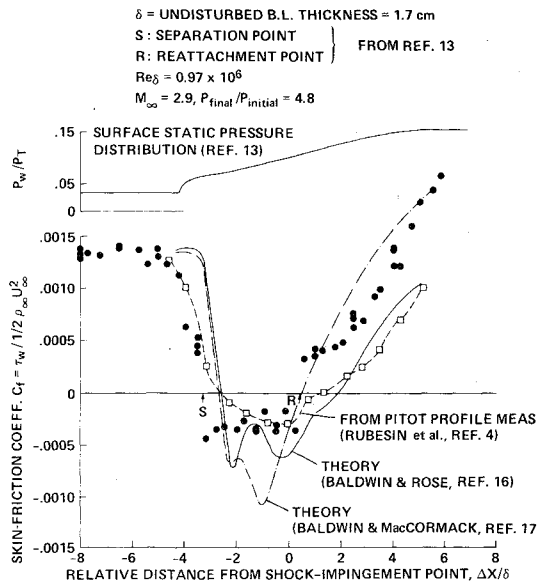


Fig. 9 Skin-friction distribution for $\alpha = 13$ deg, $M_\infty = 2.9$, $p_{final}/p_{initial} = 4.8$.

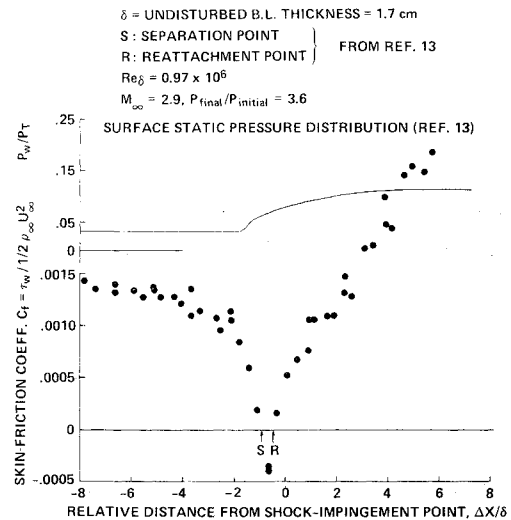


Fig. 11 Skin-friction distribution for $\alpha = 10$ deg, $M_\infty = 2.9$, $p_{final}/p_{initial} = 3.6$.

The spike at shock-impingement point remains to be understood.

Figure 9 displays the results of skin-friction measurements for the 13-deg shock generator setting that produced an extensive separation region. The present gages were not built to detect local flow direction and, hence, the measured skin-friction values were assumed to be negative in the region between the separation and reattachment points detected earlier¹³ by surface oil flow technique for the same flow setting. Figure 9 also shows the skin-friction distribution determined by Rubesin et al.⁴ from the pitot pressure profiles measured by Reda and Murphy; the analytical predictions made by Baldwin and Rose,¹⁶ using a relaxation model for the turbulent shear stress; and the prediction of Baldwin and MacCormack,¹⁷ using the eddy viscosity model with a relaxation factor. It should be noted that these latter predictions entail solution of the full time-averaged Navier-Stokes equations without any boundary-layer assumptions. It can also be seen from Fig. 9 that the present measurements show definite trends toward separation and reattachment points. The different data seem to agree well in terms of general trend, but not in actual values. Present data show a slightly increased upstream influence, as compared to Navier-Stokes solutions. Downstream of the interaction region, the present measurements indicate a tendency to higher skin-friction values, in agreement with the calculations of Baldwin and MacCormack.¹⁷ Near the separation bubble, however, it is important to realize that the flow is largely unsteady in character (see Ref. 15). The velocity in this region alternates between negative and positive values, and the present gages are not capable of discriminating between the two. Mean values of output voltage from these gages regard both positive

and negative skin-friction values as only positive, and perhaps this explains the absence of zero skin-friction readings in the present set of measurements. Away from the separation and reattachment points, the measurements are accurate; therefore, one should perhaps rely on trends to fill in the distribution close to those points. The arguments should apply to the skin-friction values inferred from pitot profiles except, of course, in the region downstream of the separation point where the analysis of Ref. 4, which uses a law-of-the-wall, may be suspect.

The rms voltage values for this setting of 13 deg are shown in Fig. 10. There is a definite increase across separation and reattachment points. But these increases do not sharply identify the separation and reattachment points, perhaps because of the flow unsteadiness of the separation bubble.

Figures 11 and 12 present the data obtained for a shock generator setting of 10 deg, for which only a very short separation bubble exists. Again the oil-flow-detected separation and reattachment points have been used as guides in interpreting these data.¹³ Trends towards these points are, however, quite impressive from the present measurements alone. As in the other cases discussed earlier, the boundary layer tends to attain significantly higher skin-friction values downstream of the interaction region.

There is some scatter of the data presented in Figs. 7-11. There are numerous potential causes of scatter of the magnitude exhibited here. First, the interaction flowfield in the wind tunnel used is inherently unsteady and may cause minor oscillations in shock-wave strength, or changes in separation and reattachment locations. Second, the data were obtained over several runs with shock generator changes in angle and streamwise location, and the scatter may simply

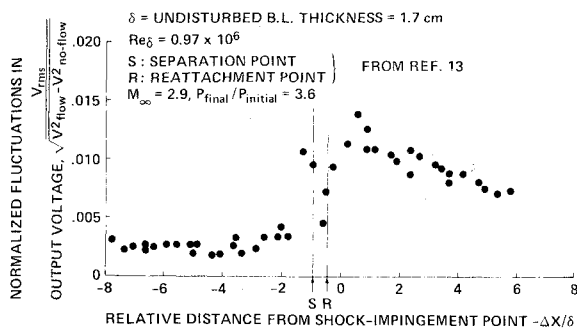


Fig. 12 Normalized fluctuations in gage outputs within interaction region, $\alpha = 10$ deg, $M_\infty = 2.9$, $p_{\text{final}}/p_{\text{initial}} = 3.6$.

represent the accuracy to which test conditions could be reset. The general level of uncertainty in these data is within 10% of the measured value. The levels of skin friction are believed to be reliable, since the reliability of the technique for fabricating gages has been established previously by measurements of skin friction on circular cylinders in crossflow.¹⁹

Concluding Remarks

This investigation of the construction, calibration, and use of buried wire gages for directly measuring skin-friction values considered several construction techniques involving various sensing materials, substrate materials, and materials to join the two. Gages made from polystyrene substrates with a solvent-bonding technique exhibited the best overall performance; they were durable and highly sensitive. Although not used for fluctuating flow measurements in this study, these gages seem to be capable of operating with an upper frequency response of about 30 kHz.

Several gages were calibrated and then used to measure skin-friction values in three turbulent boundary-layer shock-wave interactions. The measurements indicate credible trends towards separation and reattachment points, and show that the boundary layer attains significantly higher skin-friction values downstream of the interaction region than upstream. Comparisons with published results of numerical calculation techniques using various turbulent viscosity models show that complete agreement between theory and experiment is yet to be achieved. The present measurements could very well be used as a guide for developing and improving the calculation techniques.

References

- ¹Settles, G.S., Vas, I.E., and Bogdonoff, M., "Shock Wave-Turbulent Boundary Layer Interaction at a High Reynolds Number, Including Separation and Flowfield Measurements," AIAA Paper 76-164, Washington, D.C., 1976; also *AIAA Journal*, Vol. 14, Dec. 1976, pp. 1709-1715.

- ²Horstman, C.C., Kussoy, M.I., Coakley, T.J., Rubesin, M.W., and Marvin, J.G., "Shock-Wave-Induced Turbulent Boundary Layer Separation at Hypersonic Speeds," AIAA Paper 75-4, Pasadena, Calif., Jan., 1975.
- ³Mateer, G.G., Brosh, A., and Viegas, J.R., "A Normal Shock Wave-Turbulent Boundary-Layer Interaction at Transonic Speeds," AIAA Paper 76-161, Washington, D.C., 1976.
- ⁴Rubesin, M.W., Murphy, J.D., and Rose, W.C., "Wall Shear in Strongly Retarded and Separated Compressible Turbulent Boundary Layers," *AIAA Journal*, Vol. 12, Oct. 1974, pp. 1442-1444.
- ⁵Horstman, C.C., Hung, C.M., Settles, G.S., Vas, I.E., and Bogdonoff, S.M., "Reynolds Number Effects on Shock-Wave Turbulent Boundary-Layer Interactions—A Comparison of Numerical and Experimental Results," AIAA Paper 77-42, Los Angeles, Calif., 1977.
- ⁶Liepmann, H.W. and Skinner, G.T., "Shearing Stress Measurements by Use of a Heated Element," NACA 3268, Nov. 1954.
- ⁷Rubesin, M.W., Okuno, A.F., Mateer, G.G., and Brosh, A., "A Hot Wire Surface Gage for Skin Friction and Separation Detection Measurements," NASA TM X-62,465, July 1975.
- ⁸Brown, G.L., "Theory and Application of Heated Films for Skin-Friction Measurements," *Proceedings of the 1967 Heat Transfer and Fluid Mechanics Institute*, Stanford Univ. Press, Stanford, Calif., 1967, pp. 361-381.
- ⁹Bellhouse, B.J. and Schultz, D.L., "Determination of Skin Friction, Separation and Transition with a Thin Film Heated Element," RAE Reports and Memoranda No. 3445, Feb. 1964.
- ¹⁰Bellhouse, B.J. and Schultz, D.L., "The Measurement of Skin Friction in Supersonic Flow by Means of Heated Thin Film Gages," Aeronautical Research Council, ARC R&M 3490, 1968.
- ¹¹Owen, F.K. and Bellhouse, B.J., "Skin-Friction Measurements at Supersonic Speeds," *AIAA Journal*, Vol. 8, July 1970, pp. 1358-1360.
- ¹²McCroskey, W.J. and Durbin, E.J., "Flow Angle and Shear Stress Measurements Using Heated Films and Wires," *Journal of Basic Engineering, Transactions of ASME*, Vol. 94, Jan. 1972, pp. 46-52.
- ¹³Reda, D.C. and Murphy, J.D., "Shock Wave-Turbulent Boundary-Layer Interactions in Rectangular Channels," AIAA Paper 72-715, Boston, Mass., 1972.
- ¹⁴Modarress, D. and Johnson, D.A., "Investigation of Shock Induced Separation of a Turbulent Boundary Layer Using Laser Velocimetry," AIAA Paper 76-374, San Diego, Calif., 1976.
- ¹⁵Bachalo, W.D., Modarress, D., and Johnson, D.A., "Experiments on Transonic and Supersonic Turbulent Boundary-Layer Separation," AIAA Paper 77-47, Los Angeles, Calif., 1977.
- ¹⁶Baldwin, B.S. and Rose, W.C., "Calculation of Shock Separated Boundary Layers," *Proceedings of Conference on Aerodynamic Analysis Requiring Advanced Computers*, Langley Research Center, Mar. 4-6, 1976, pp. 401-411.
- ¹⁷Baldwin, B.S. and McCormack, R.W., "Modifications of the Law of the Wall and Algebraic Turbulence Modelling for Separated Boundary Layers," AIAA Paper 76-350, San Diego, Calif., 1976.
- ¹⁸Murphy, J.D. and Davis, C.B., "Users Guide—Ames Inlet Boundary Layer Program MK I," NASA TM X-62,211, Jan. 1973.
- ¹⁹Murthy, V.S. and Rose, W.C., "Form Drag, Skin Friction, and Vortex Shedding Frequencies for Subsonic and Transonic Crossflows on a Circular Cylinder," AIAA Paper 77-687, Albuquerque, N. Mex., 1977.